51st IEEE Conference on Decision and Control
December 10-13, 2012. Maui, Hawaii, USA

Steady-state performance optimization for variable-gain motion control using extremum seeking*

B.G.B. Hunnekens[1], M.A.M. Haring[2], N. v.d. Wouw[1] and H. Nijmeijer[1]

Abstract— **In this paper, we employ an extremum-seeking control strategy for steady-state performance optimization of variable-gain controllers for linear motion systems. Variable-gain control can balance the tradeoff between low-frequency disturbance suppression and sensitivity to high-frequency noise in a more desirable manner than linear controllers can. However, the optimal performance-based tuning of the variable-gain controller parameters is far from trivial. A model-based performance optimization method would require an accurate disturbance model, which may be hard to obtain in practice. The extremum-seeking controller proposed here does not require any plant- or disturbance model and therewith circumvents this difficulty. To illustrate the results, the variable-gain controller of a short-stroke wafer stage of a wafer scanner is optimized using extremum-seeking control.**

I. INTRODUCTION

Linear motion systems are still often controlled by linear controllers, mostly of the proportional-integral-differential (PID) type. However, it is well known that linear controllers suffer from inherent performance limitations such as the waterbed effect [3]. This waterbed effect describes the well-known tradeoff between low-frequency tracking and sensitivity to high-frequency disturbances and measurement noise. If only low-frequency disturbances are present, a high-gain controller is preferred in order to obtain good low-frequency tracking properties. On the other hand, if only high-frequency disturbances and noise are present, a low-gain controller is preferred as not to amplify the high-frequency disturbances. Typically, a linear controller needs to balance between these two conflicting objectives with the waterbed effect as a constraint due to the Bode sensitivity integral.

To overcome such a performance limitation to a certain extent, a nonlinear variable-gain control strategy has been employed in [8], [7], [18]. In these references, it has been shown that variable-gain controllers have the capability of outperforming linear controllers. Although the controller designs are intuitive in nature, an optimal performance-based tuning of such variable-gain controllers is far from trivial and sub-optimal tuning is typically done in an heuristic fashion.

One way to optimize the performance of the variable-gain controller for a certain disturbance situation, is to pursue a model-based approach. However, this requires the modeling of the disturbances that act on the system, which is typically considered a difficult task in a motion control setting. To circumvent the need for disturbance modeling, we propose to use an extremum-seeking control approach to optimally tune the variable-gain controller parameters. The benefits of the adaptive tuning of variable-gain controller parameters have been shown in an iterative feedback tuning context in [6].

Extremum-seeking control is an adaptive control approach that optimizes a certain performance measure in terms of the steady-state output of a system in real-time, by automated continuous tuning of the system parameters. Since only output measurements of the plant are used, no knowledge on the plant dynamics and disturbances is required. In general, extremum-seeking control is typically used to optimize plants with constant steady-state outputs [1], [9], [15], [14]. Recently, an extremum-seeking control method has been proposed for steady-state performance optimization of general nonlinear plants with arbitrary periodic steady-state outputs of the plant [4], [5]. In a motion control context, we often encounter such periodic steady-state behavior due to the presence of periodic setpoints.

The contribution of this paper is the performance-based tuning of variable-gain controllers for linear motion systems, using this extremum-seeking control, without using a disturbance model. In particular, we show how this strategy can be employed to optimize the performance of a variable-gain controlled short-stroke wafer stage of a wafer scanner.

The remainder of the paper is organized as follows. In Section II, we introduce the variable-gain control strategy and present easy-to-check conditions for the global exponential stability of the closed-loop steady-state solutions. The extremum-seeking control strategy that is used in this paper will be introduced in Section III. The application of this strategy to the performance optimization of the variable-gain controlled short-stroke wafer stage will be discussed in Section IV. Conclusions are presented in Section V.

II. VARIABLE GAIN CONTROL

Consider the variable-gain controller structure depicted in Fig. 1, with the underlying linear control structure consisting of the plant and nominal linear controller with transfer functions $P(s)$ and $C(s)$, $s \in \mathbb{C}$ respectively, reference signal r, force disturbance f, and error signal e. To enhance the performance of the linear controller $C(s)$, we introduce a nonlinearity $\varphi(e)$ and filter $F(s)$. The choice of the shape of the nonlinearity $\varphi(e)$ is given by a dead-zone characteristic

$$\varphi_(e) = \begin{cases} \alpha(e+\delta) & \text{if } e < -\delta, \\ 0 & \text{if } |e| \leq \delta, \\ \alpha(e-\delta) & \text{if } e > \delta, \end{cases} \tag{1}$$

*This research is financially supported by the Dutch Technology Foundation STW.

[1]B.G.B. Hunnekens, N. van de Wouw, and H. Nijmeijer are with the Eindhoven University of Technology, Department of Mechanical Engineering, P.O. Box 513, NL 5600 MB Eindhoven, The Netherlands B.G.B.Hunnekens@tue.nl

[2]M.A.M. Haring is with the Norwegian University of Science and Technology, Department of Engineering Cybernetics, 7491 Trondheim, Norway.

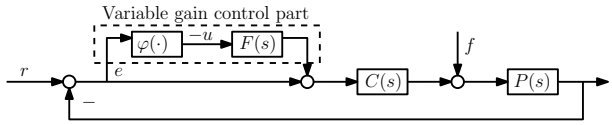

Fig. 1. Closed-loop variable-gain control scheme.

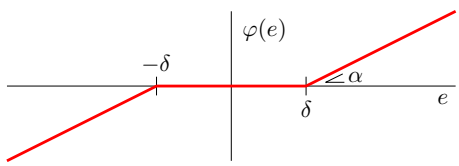

Fig. 2. Nonlinearity $\varphi(e)$ discriminating between small errors and large errors.

see Fig. 2, and is key in to our variable-gain controller design. Typically, in motion systems, errors induced by low-frequency disturbances are larger in amplitude than those induces by high-frequency disturbances [16]. Therefore, if the error signal $e(t)$ exceeds the pre-defined dead-zone level δ, an additional controller gain α is induced, yielding superior low-frequency tracking and disturbance suppression properties. If, however, the error signal does not exceed the dead-zone length δ, no additional gain is induced as not to avoid the deterioration of the sensitivity to high-frequency disturbances.

Due to the choice of the variable-gain control structure in Fig. 1, the closed-loop dynamics can be modeled as a Lur'e-type system of the form

$$\dot{x} = Ax + Bu + B_w w(t) \tag{2}$$
$$e = Cx + D_w w(t) \tag{3}$$
$$u = -\varphi(e), \tag{4}$$

where $w(t) \in \mathbb{R}^m$ contains all external inputs, such as the reference $r(t)$ and force disturbance $f(t)$. The transfer function $G_{eu}(s)$ denotes the transfer from input $u \in \mathbb{R}$ to output $e \in \mathbb{R}$, see Fig. 1, and can be expressed as

$$G_{eu}(s) = C(sI - A)^{-1}B = \frac{P(s)C(s)F(s)}{1 + P(s)C(s)}. \tag{5}$$

In this paper, we consider the case of periodic disturbances $w(t)$, which, in a motion control context, are often present due to periodicity of setpoints. The following theorem provides conditions under which system (2)-(4), excited by a T-periodic input $w(t)$, has a uniquely defined T-periodic globally exponentially stable steady-state solution.

Theorem II.1 *[17], [16] Consider system* (2)-(4). *Suppose*

A1 The matrix A is Hurwitz;

A2 The nonlinearity $\varphi(e)$ satisfies:

$$0 \leq \frac{\varphi(e_2) - \varphi(e_1)}{e_2 - e_1} \leq \alpha, \tag{6}$$

for all $e_1, e_2 \in \mathbb{R}$, $e_1 \neq e_2$;

A3 The transfer function $G_{eu}(s)$ given by (5) *satisfies*

$$\sup_{\omega \in \mathbb{R}} |G_{eu}(i\omega)| > -\frac{1}{\alpha}. \tag{7}$$

Then for any T-periodic piecewise continuous input $w(t)$, system (2)-(4) *has a unique T-periodic solution $\bar{x}_w(t)$, which is globally exponentially stable and bounded for all $t \in \mathbb{R}$.*

We will call $\bar{x}_w(t)$ the steady-state solution. Systems with such a uniquely defined globally exponentially stable steady-state solution (for arbitrary bounded inputs $w(t)$) are called exponentially convergent, see e.g. [2], [12].

Note that the maximum allowable value of the additional gain α is determined by the frequency-domain condition (7). The dead-zone length δ is typically chosen in an heuristic fashion [7], [8]. Here, we aim to tune the dead-zone length δ in order to optimize the performance. One could opt to use a model-based approach and optimize the variable-gain controller using a model of the system and disturbances. However, although for motion systems accurate plant models (which can be obtained via frequency response measurements) are typically available, accurate disturbance models are very difficult to obtain. To avoid the need for such disturbance models, we propose to tune the dead-zone length δ using an extremum-seeking control approach, which does not use any knowledge on the disturbances (or plant model). First, the extremum-seeking control strategy for nonlinear systems with periodic steady-state outputs, as introduced in [4], [5], will be discussed in Section III. Subsequently, the approach will be applied to a variable-gain controlled wafer stage in Section IV.

III. EXTREMUM SEEKING CONTROL FOR PERIODIC STEADY-STATES

Extremum-seeking control is commonly used to optimize plants with constant steady-state outputs [1], [9], [15], [14]. Extremum-seeking control for plants with time-varying outputs has received relatively little attention. In [4], [5], an extremum-seeking scheme has recently been proposed for the optimization of nonlinear plants with *periodic* steady-state outputs, which is relevant in the scope of tracking and disturbance rejection problems for motion systems, as we will see in Section IV.

Consider the extremum-seeking scheme shown in Fig. 3, which, in the spirit of [10], consists of a stabilized plant (2)-(4), a performance output y, a cost function with output q, a derivative estimator and an optimizer. Let us elaborate on the different elements in this extremum-seeking scheme in the scope of the motion control setting specified in the previous section; for more details we refer to [4], [5]:

- We aim to find the value of δ that optimizes, in a certain sense, a steady-state performance output $\bar{y}_w(t, \delta)$ of the stabilized plant (2)-(4). In order to do so, the performance of the variable-gain controller is characterized by the cost function

$$q(t, \delta) = \int_{t-T}^{t} h(s(\tau), y(\tau, \delta))d\tau, \tag{8}$$

where $y = e$, since in our motion control context, the tracking error e is the important performance variable. The T-periodic function $s(t)$ is a selection function allowing to weigh only certain errors in an important

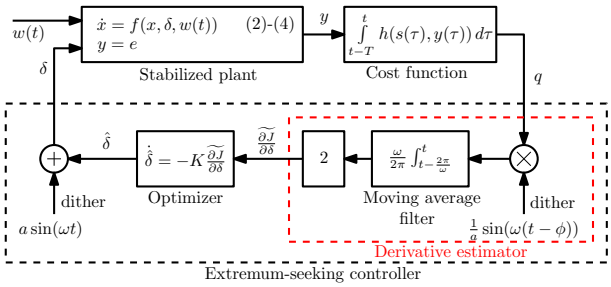

Fig. 3. Extremum-seeking scheme for optimal tuning of deadzone length δ.

performance window (see Section IV for more details). Note that the output of the performance cost function q as in (8) is constant if $e(t, \delta)$ is T-periodic in t, for fixed δ;

- The derivative estimator uses dither to obtain an estimate $\widetilde{\partial J}/\partial\delta$ of the true gradient $\partial J/\partial\delta$ of the unknown steady-state performance map

$$J(\delta) = \int_0^T h(s(t), \bar{y}_w(t, \delta))dt, \tag{9}$$

i.e. the performance map for fixed δ and steady-state error $\bar{e}_w(t, \delta) = \bar{y}_w(t, \delta)$;

- The extremum-seeking controller aims to find the minimum of the unknown steady-state performance map $J(\delta)$, which we assume to be attained at δ^*;
- The estimated gradient $\widetilde{\partial J}/\partial\delta$ is used by the optimizer

$$\dot{\hat{\delta}} = -K \widetilde{\frac{\partial J}{\partial \delta}}, \tag{10}$$

in order to steer the nominal value $\hat{\delta}$ of the dead-zone length δ towards the optimal performance optimizing value δ^*, where

$$\delta = \hat{\delta} + a \sin(\omega t), \tag{11}$$

with a the dither amplitude, and ω the dither frequency;

- The moving average filter is used to filter out the oscillations with frequency ω in the performance q, resulting in a more accurate gradient estimate $\widetilde{\partial J}/\partial\delta$ compared to using low-pass and/or high-pass filters as applied in e.g. [15]. The phase shift $\omega\phi$ in the dither $\frac{1}{a}\sin(\omega(t-\phi))$ is introduced to compensate for the delays introduced by the plant dynamics and the performance measure in (8) and can be used to improve the gradient estimate.

In essence, the following essential assumptions are made in [4], [5] to guarantee the stability of the above extremum-seeking scheme:

B1 The disturbances $w(t)$ are bounded, T-periodic disturbances with a known constant period T;

B2 For all *fixed* parameters $\delta \in \mathbb{R}$, the nonlinear system (2)-(4) exhibits a unique globally asymptotically stable steady-state solution $\bar{x}_w(t, \delta)$, with the same period time T;

B3 The sufficiently smooth steady-state performance map $J(\delta)$ has a unique global minimum at δ^*.

Under these assumptions, it is shown in Theorem 5.26 in [4] (or Theorem 19 in [5]) that the extremum-seeking scheme in Fig. 3 is semi-globally practically asymptotically stable (SGPAS). Loosely speaking, such a SGPAS property guarantees that there exist sufficiently small values for the dither amplitude a, dither frequency ω, and extremum-seeking gain K, such that the closed-loop extremum-seeking scheme converges to an arbitrarily small neighborhood of the performance-optimizing value δ^* (for arbitrarily large sets of initial conditions). Hence, by proper selection of the parameters a, ω, and K, we can assure that the optimal steady-state performance of the plant is approached as closely as desired.

Remark III.1 Note that Assumption B2 is in a certain sense the counterpart of the assumption of a unique globally asymptotically stable equilibrium point in the scope of extremum-seeking control for plants with *constant* steady-state outputs, see e.g. [15]. Note that the conditions of Theorem II.1 guarantee that Assumption B2 is satisfied. Indeed, the stabilized plant will then have a unique, T-periodic, globally exponentially stable steady-state solution $\bar{x}_w(t, \delta)$ for fixed δ and T-periodic inputs $w(t)$. Note that this property guarantees the existence and uniqueness of the steady-state performance map $J(\delta)$, see [13].

Remark III.2 Note that the inclusion of the selection function $s(t)$ in the definition of the performance cost function (8) was not included in [4], [5]. However, since the selection function $s(t)$ is also periodic with period time T, the function $h(s(t), \bar{y}_w(t, \delta))$ in (8) is also periodic in t with period time T, for fixed δ, and is, moreover, bounded for bounded x and $w(t)$. Therefore, the output of the cost function q will still be constant if the steady-state error $\bar{e}_w(t, \delta)$ is T-periodic, such that the results in [4], [5] can be directly employed.

IV. APPLICATION TO THE MOTION CONTROL OF A WAFER STAGE

In this section, we will use the extremum-seeking controller discussed in Section III to optimize the performance of a variable-gain controller for the motion control of a short-stroke wafer stage of a wafer scanner, see Fig. 4, which is disturbed by force disturbances. Wafer scanners are used to produce integrated circuits (IC's). Light, emitted by a laser, falls on a reticle, which contains an image. This image is projected onto a wafer by passing through a lens. Due to this illumination process, in combination with a photoresist, a chemical reaction takes place which results in an image on the wafer, containing the IC's. This process requires positioning of the wafer stage in three degrees of freedom (x, y and z) with nanometer-accuracy. We will focus on the z-direction, see Fig. 4, which should be kept in focus because of the illumination process, while aggressive motion in the horizontal x- and y-direction disturb the vertical z-direction due to mechanical crosstalk.

High-bandwidth linear controllers are used to achieve the desired motion. Due to the waterbed-effect [3], low-frequency performance improvement (i.e. a higher bandwidth) goes hand in hand with high-frequency performance deterioration. Variable gain control can be used to balance this trade-off in a more desirable manner [8], [7]. However,

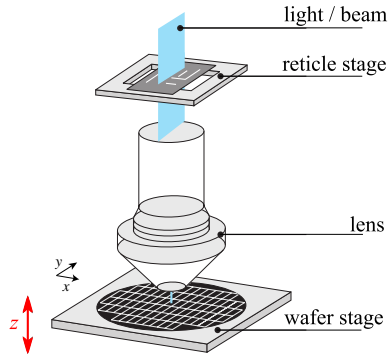

Fig. 4. The z-direction of the wafer-stage will be controlled by a variable-gain controller.

the performance-based tuning of the variable-gain controller parameters is a challenging task. Here, we propose to tune the dead-zone length δ of the variable-gain controller, see Fig. 2, using the extremum-seeking approach described in Section III. Note that the extremum-seeking approach does not require a detailed disturbance model.

A. Model specification of the wafer stage

The plant dynamics are modeled by the transfer function

$$P(s) = \frac{m_1 s^2 + bs + k}{s^2(m_1 m_2 s^2 + b(m_1+m_2)s + k(m_1+m_2))}, \tag{12}$$

$s \in \mathbb{C}$, where the following numerical values are used for the plant model [8]: $m_1 = 5$ kg, $m_2 = 17.5$ kg, $k = 7.5 \cdot 10^7$ N/m, $b = 90$ Ns/m. The nominal low-gain ($\alpha = 0$) controller $C(s) = C_{PID}(s)C_{lp}(s)C_n(s)$ consists of a PID controller $C_{PID}(s)$, a second-order low-pass filter $C_{lp}(s)$ and a notch filter $C_n(s)$ to suppress the plant resonance. The filters are given by: $C_{PID}(s) = (k_p(s^2 + (\omega_i + \omega_d)s + \omega_i\omega_d))/(\omega_d s)$, where $k_p = 6.9 \cdot 10^6$ N/m, $\omega_d = 3.8 \cdot 10^2$ rad/s, and $\omega_i = 3.14 \cdot 10^2$ rad/s; $C_{lp}(s) = \omega_{lp}^2/(s^2 + 2\beta_{lp}\omega_{lp}s + \omega_{lp}^2)$, where $\omega_{lp} = 3.04 \cdot 10^3$ rad/s, and $\beta_{lp} = 0.08$; $C_n(s) = (\omega_p/\omega_z)^2(s^2 + 2\beta_z\omega_z s + \omega_z^2)/(s^2 + 2\beta_p\omega_p s + \omega_p^2)$, where $\omega_p = 5.03 \cdot 10^3$ rad/s, $\beta_p = 0.88$, $\omega_z = 4.39 \cdot 10^3$ rad/s, and $\beta_z = 2.7 \cdot 10^{-3}$. The loop-shaping filter $F(s)$ is given by $F(s) = (\omega_{p,F}/\omega_{z,F})^2(s^2 + 2\beta_{z,F}\omega_{z,F}s + \omega_{z,F}^2)/(s^2 + 2\beta_{p,F}\omega_{p,F}s + \omega_{p,F}^2)$, with $\omega_{p,F} = \omega_{z,F} = 2000$ rad/s, $\beta_{p,F} = 4.8$, and $\beta_{z,F} = 0.6$. Note that these filters define the transfer function $G_{eu}(s)$ in (5).

In the following, we will specify a disturbance model. We stress here that this disturbance model is introduced solely for simulation purposes, the extremum-seeking controller does not use this disturbance model.

The z-direction of the wafer stage should be kept in focus, therefore we need to track a zero-reference signal $r(t) = 0$. Force-disturbances $f(t)$, see Fig. 1, are a dominant source of disturbances for the z-direction of the wafer stage. These force disturbances can be considered to have two main contributions $u_{FFz}(t)$ and $u_p(t)$, such that

$$f(t) = u_{FFz}(t) + u_p(t), \tag{13}$$

where $u_{FFz}(t)$ is a mainly low-frequency contribution (below the bandwidth), and $u_p(t)$ is a high-frequency contribution (above the bandwidth).

Low-frequent force disturbance u_{FFz}. Because the wafer stage is undergoing large accelerations in the horizontal x- and y-direction (around 28.5 m/s^2), the feed-forward forces acting in the horizontal plane to realize such setpoints affect the z-direction due to unavoidable mechanical cross-talk. Based on a 3rd-order polynomial reference signal $x_d(t)$ in the x-direction, the force-disturbance u_{FFz} in the z-direction is modeled in the following way: the reference trajectory x_d is filtered by a feed-forward filter $FF_x(s)$ which transforms the position x_d to a feed-forward force u_{FFx} in the x-direction, and a static cross-talk factor γ_{ct} is used ($\gamma_{ct} = 4.5 \cdot 10^{-2}$, based on experimental data) to link the feed-forward force u_{FFx} in x-direction to the force disturbance u_{FFz} in z-direction. The filter $FF_x(s)$ is given as a 2nd-order high-pass filter $FF_x(s) = (\omega_{hp}^2 s^2)/(s^2 + 2\beta_{hp}\omega_{hp}s + \omega_{hp}^2)$, where $\omega_{hp} = 400\pi$ rad/s, and $\beta_{hp} = 0.5$. All IC's contained on a wafer are illuminated in the same way, over a scanning length L with scanning velocity V. This leads to periodic motion profiles that need to be carried out by the wafer stage in the horizontal (x-y)-plane. The T-periodic 3rd-order reference signal $x_d(t)$ is parameterized corresponding to values for maximum jerk and acceleration used in practice: $j_{max} = 3000$ m/s^3, and $a_{max} = 28.35$ m/s^2. The setpoint $x_d(t)$, consisting of subsequent acceleration, constant velocity, and deceleration phases, see Fig. 5, is fully determined by the scanning velocity V and scanning length L. Typical values for these parameters are $V = 0.5$ m/s and $L = 40 \cdot 10^{-3}$ m, resulting in a period-time of $T = 0.29$ s. The constant velocity part consists of the scan time $T_{scan} = L/V$, a settling time $T_{set} = 2 \cdot 10^{-3}$ s, and a time $T_{win} = 0.011$ s needed to open a 'diaphragm'. Note that the scanning is repeated such that the force disturbance u_{FFz} is periodic with period time T.

High-frequent force disturbance u_p. The sources of the high-frequency disturbance are amplifier noise, and possibly other high-frequency disturbances such as e.g. perturbations stemming from the immersion process taking place on the wafer stage. Although a possible noisy perturbation signal stemming from either of the above sources is in general not periodic, we can very well approximate these disturbances as being periodic with period time T of the set-point induced force disturbance u_{FFz}. Note that this assumption can be justified if the noisy disturbances are of a significantly higher frequency (200-400 Hz) than the frequency $1/T$ of the signal $u_{FFz}(t)$. This is indeed the case in practice and more numerical specifics will be given later. Moreover, it is well worth adopting such a modeling of the high-frequency noise because it allows for an explicit quantification of the steady-state performance. For the purpose of simulation, we model the high-frequency noise as a sum of N_p sinusoidal signals of constant amplitude A_p, frequencies $\omega_{p,j}$ and random phase angles $\phi_{p,j}$ such that

$$u_p(t) = \sum_{j=1}^{N_p} A_p \sin(\omega_{p,j}t + \phi_{p,j}), \tag{14}$$

where $N_p = 50$, and $A_p = 0.12$ N, based on experiments, and the phase $\phi_{p,j} \in [0, 2\pi]$ is chosen randomly. The N_p

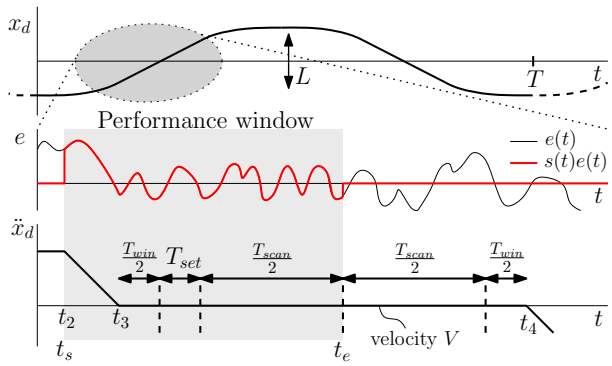

Fig. 5. Weighting interval for the performance objective J.

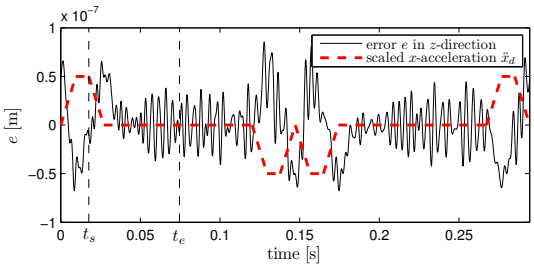

Fig. 6. Typical steady-state error response (one period).

frequencies in the signal are chosen as multiples of $1/T$ (≈ 3 Hz) in the range 200-400 Hz such that the total force disturbance $f(t)$ is a periodic signal with period time T.

A typical steady-state error response $\bar{e}_w(t,\delta)$ of the short-stroke wafer stage subjected to the force-disturbances described in this section, is shown in Fig. 6. Note the low-frequency contributions, due to the force cross-talk $u_{FFz}(t)$ coming from acceleration $\ddot{x}_d$ in x-direction of the setpoint, see the dashed line in Fig. 6, and the high-frequency contributions due to the noise $u_p(t)$.

B. Performance quantification for the wafer stage

A typical performance objective (8) for a motion system is the minimization of the error in a certain important time window $[t_s, t_e]$ during each period:

$$q(t,\delta) = \frac{1}{t_e - t_s}\int_{t-T}^{t} s(\tau)e^2(\tau,\delta)d\tau, \qquad (15)$$

where t_s and t_e are the starting time and ending time of the time interval, respectively. Note that the minimization of (15) corresponds to our motion control goal of minimizing the tracking error in an important performance window and relates to commonly used performance quantifiers as the moving average (related to machine overlay) and moving standard deviation (related to imaging) used in wafer scanner systems [6]. Other choices of signal norms are also possible, see [4], [5]. In the context of the motion control of the wafer stage, we aim to optimize this performance in the important performance window indicated in Fig. 5, which is located around the time-instance where scanning starts. Note that the T-periodic selection window

$$s(t) = \begin{cases} 1 & \text{if } t \in [t_s, t_e] + kT, k \in [0,1,\ldots], \\ 0 & \text{otherwise,} \end{cases} \qquad (16)$$

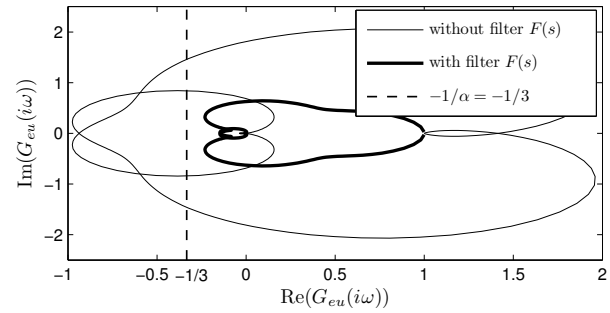

Fig. 7. Frequency-domain condition $\mathrm{Re}(G_{eu}(i\omega)) > -1/\alpha \ \forall \omega \in \mathbb{R}$.

see Section III, selects the performance-relevant part of the error $e(t,\delta)$, as is indicated in Fig. 5 and in (15).

C. Performance optimization using extremum-seeking

Before applying the extremum-seeking controller to tune the dead-zone length δ, we should verify that Assumptions B1-B3 for SGPAS of the extremum-seeking scheme are satisfied, see Section III. Since we consider a periodic and bounded force disturbance $f(t)$, Assumption B1 is satisfied; moreover, as we will see, Assumption B3 is satisfied for the range of values of δ that we are interested in. Assumption B2 can easily be checked by verifying the conditions of Theorem II.1, see Remark III.1. Using the model specified in Section IV-A, we can easily verify that the matrix A (or equivalently, the transfer function $G_{eu}(s)$ in (5)) is Hurwitz (by the design of the linear loop-shaped controller $C(s)$ the linear closed-loop $P(s)C(s)/(1+P(s)C(s))$ is Hurwitz, and, additionally, filter $F(s)$ is Hurwitz) such that condition A1 of Theorem II.1 is satisfied. The dead-zone nonlinearity $\varphi(e)$, see Fig. 2, satisfies the incremental sector condition (6), such that condition A2 of Theorem II.1 is satisfied. From Fig. 7, it is clear that the frequency-domain condition A3 of Theorem II.1 is satisfied for $\alpha = 3$. Note that this figure also illustrates the reason for including the filter $F(s)$ in the variable-gain controller. Since all conditions of Theorem II.1 are satisfied, system (2)-(4) exhibits a unique bounded globally exponentially stable T-periodic steady-state solution for *fixed* δ, such that Assumption B2 is satisfied. Note that this also guarantees the existence and uniqueness of the steady-state performance map $J(\delta)$ in (9).

In order to validate the convergence of the extremum-seeking controller to the optimal dead-zone length δ^*, we calculate the steady-state performance map $J(\delta)$ for a range of values of δ. We can do this in a computationally efficient manner using the so-called Mixed-Time-Frequency algorithm introduced in [11]. The result is shown in Fig. 8 with the dashed line, which verifies that Assumption B3 is satisfied for the domain of interest. The extremum-seeking controller described in Section III is applied with the following settings: the initial dead-zone length $\hat{\delta} = 4$ nm, dither amplitude $a = 1$ nm, dither frequency $\omega = 4$ rad/s, extremum-seeking gain $K = 0.2$, and zero initial conditions for all the states. The extremum-seeking controller is turned on (K is set from 0 to 0.2) at $t = 2$ s. The simulation results are shown in Fig. 8, which illustrates the fact that the dead-zone length δ of the variable-gain controller

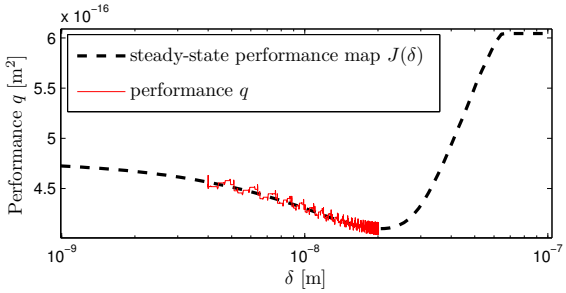

Fig. 8. Performance optimization of variable-gain controller using extremum-seeking controller.

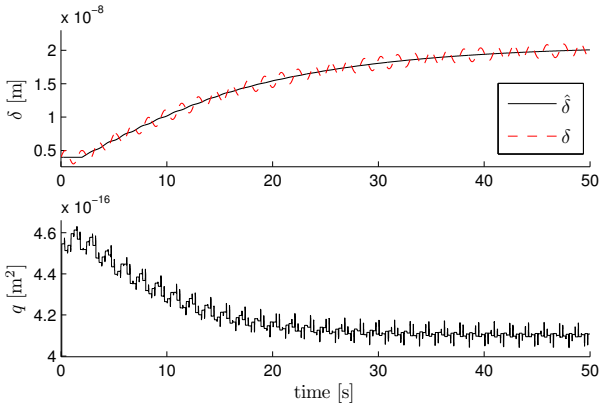

Fig. 9. Convergence of dead-zone length δ and performance q.

converges to a small neighborhood of the optimal value $\delta^* \approx 20$ nm. Fig. 9 shows the nominal signal $\hat{\delta}$ and the signal $\delta = \hat{\delta} + a\sin(\omega t)$, which includes the dither, and the performance q as a function of time. The minimization of q indicates that we minimize the integral of the squared error in an important time-window located around the time-instance where scanning starts, see (15). Note that the variable-gain controller outperforms the linear low-gain controller ($\delta = \infty$) by 15% and high-gain controller ($\delta = 0$ nm) by 35 %, see Fig. 8, which is very significant in this type of nanometer accuracy motion control applications.

Note that by a proper tuning of the extremum-seeking parameters a, ω and K, the neighborhood of δ^* to which the extremum-seeking controller converges can be decreased, but at the cost of a lower transient convergence speed.

Remark IV.1 In [4], [5], it is actually assumed that the dynamics $f(x, \delta, w)$, see Fig. 3, is twice continuously differentiable with respect to δ. However, the use of the dead-zone nonlinearity $\varphi(e)$ as shown in Fig. 2 violates this smoothness assumption. It is possible to define a sufficiently smooth variant of $\varphi(e)$ which can arbitrarily closely approximate the dead-zone nonlinearity. For reasons related to the ease of implementation of a non-smooth piecewise linear dead-zone characteristic, we used the dead-zone nonlinearity as shown in Fig. 2 which does still lead to convergence of the extremum-seeking scheme, as shown in this section.

V. CONCLUSIONS

In this paper we have proposed an adaptive strategy for optimization of the steady-state performance of a variable-gain motion controller based on extremum-seeking control. The extremum-seeking control approach allows to tune the parameter of the nonlinear controller, without using explicit knowledge on the disturbances present. This paper shows the importance and practical applicability of the extremum-seeking control scheme for nonlinear systems with time-varying periodic steady-state outputs. An application of a variable-gain controlled short-stroke wafer stage model of a wafer scanner has been presented to illustrate the effectiveness of the extremum-seeking control strategy. Moreover, it has been shown that the resulting optimal variable-gain controller outperforms linear motion controllers.

REFERENCES

[1] K.B. Ariyur and M. Krstić. *Real-time optimization by extremum-seeking control*. Wiley-Interscience, Hoboken, NJ, 2003.

[2] B.P. Demidovich. Dissipativity of a nonlinear system of differential equations. *Ser. Mat. Mekh.*, Part I-6:19–27, 1961.

[3] J. Freudenberg, R. Middleton, and A. Stefanopoulou. A survey of inherent design limitations. In *Proc. of the American Control Conference*, pages 2987–3001, Chicago, Illinois, 2000.

[4] M.A.M. Haring. Extremum-seeking control for steady-state performance optimization of nonlinear plants with periodic steady-state outputs. Technical Report DC2011.029, Eindhoven University of Technology, Eindhoven, The Netherlands, 2011. Available at *http://www.dct.tue.nl/New/Wouw/TechReportDC2011029.pdf*.

[5] M.A.M. Haring, N. v.d. Wouw, and D. Nešić. Extremum-seeking control for nonlinear systems with periodic steady-state outputs. Submitted, 2012.

[6] M. Heertjes, T. Tepe, and H. Nijmeijer. Multi-variable iterative tuning of a variable gain controller with application to a scanning stage system. In *2011 American Control Conference, ACC 2011*, pages 816–820, San Francisco, CA, 2011.

[7] M.F. Heertjes and G. Leenknegt. Switching control in blu-ray disk drives. *Mechatronics*, 20:453–463, 2010.

[8] M.F. Heertjes, X.G.P. Schuurbiers, and H. Nijmeijer. Performance-improved design of N-PID controlled motion systems with application to wafer stages. In *IEEE Transactions on Industrial Electronics*, volume 56 (5), pages 1347–1355, 2009.

[9] M. Krstić and H.-H. Wang. Stability of extremum seeking feedback for general nonlinear dynamic systems. *Automatica*, 36(4):595–601, 2000.

[10] D. Nešić, Y. Tan, W.H. Moase, and C. Manzie. A unifying approach to extremum seeking: Adaptive schemes based on estimation of derivatives. In *2010 49th IEEE Conference on Decision and Control, CDC 2010*, pages 4625–4630, Atlanta, GA, 2010.

[11] A. Pavlov and N. Van De Wouw. Fast computation of frequency response functions for a class of nonlinear systems. In *47th IEEE Conference on Decision and Control, CDC 2008*, pages 1180–1186, Cancun, Mexico, 2008.

[12] A. Pavlov, N. van de Wouw, and H. Nijmeijer. *Uniform output regulation of nonlinear systems: a convergent dynamics approach*. Boston: Birkhäuser, 2005.

[13] A. Pavlov, N. van de Wouw, and H. Nijmeijer. Frequency response functions for nonlinear convergent systems. *IEEE Trans Autom Control*, 52(6):1159–1165, 2007.

[14] Y. Tan, W.H. Moase, C. Manzie, D. Nešić, and I.M.Y. Mareels. Extremum seeking from 1922 to 2010. In *Proceedings of the 29th Chinese Control Conference*, 2010.

[15] Y. Tan, D. Nešić, and I. Mareels. On non-local stability properties of extremum seeking control. *Automatica*, 42(6):889–903, 2006.

[16] N. van de Wouw, H.A. Pastink, M.F. Heertjes, A.V. Pavlov, and H. Nijmeijer. Performance of convergence-based variable-gain control of optical storage drives. *Automatica*, 44:15–27, 2008.

[17] V.A. Yakubovich. The matrix inequality method in the theory of the stability of nonlinear control systems - I. The absolute stability of forced vibrations. *Automation and Remote Control*, 7:905–917, 1964.

[18] J. Zheng, G. Guo, and Y. Wang. Nonlinear PID control of linear plants for improved disturbance rejection. *16th IFAC World Congress (IFAC 2005)*, Prague, 2005.